ISSN 0016-8521, Geotectonics, 2016, Vol. 50, No. 2, pp. 179–195. © Pleiades Publishing, Inc., 2016.
Original Russian Text © M.D. Khutorskoi, B.G. Polyak, 2016, published in Geotektonika, 2016, No. 2, pp. 43–61.

Role of Radiogenic Heat Generation in Surface Heat Flow Formation

M. D. Khutorskoi and B. G. Polyak

Geological Institute, Russian Academy of Sciences, Pyzhevskii per. 7, Moscow, 119017 Russia

e-mail: mkhutorskoy@ginras.ru

Received April 26, 2015

Abstract—Heat generation due to decay of long-lived radioactive isotopes is considered in the Earth's crust of the Archean–Proterozoic and Paleozoic provinces of Eurasia and North America. The heat flow that forms in the mantle is calculated as the difference between the heat flow observed at the boundary of the solid Earth and radiogenic heat flow produced in the crust. The heat regime in regions with anomalously high radiogenic heat generation is discussed. The relationship between various heat flow components in the Precambrian and Phanerozoic provinces has been comparatively analyzed, and the role of erosion of the surface-heat-generating layer has been estimated.

Keywords: geothermics, crust, mantle, heat flow, radiogenic heat generation, erosion

DOI: 10.1134/S0016852116020047

INTRODUCTION

The nature of heat flow (HF) from the Earth's interior is the main object of geothermics. Before the phenomenon of radioactivity was discovered, its nature was related to cooling of the once molten planet. After this discovery, the role of radiogenic heat generation has been regarded as crucial. Nowadays it is thought that various sources participate in the production of intraterrestrial heat and their role is time-dependent.

Radiogenic heat generation (RHG) in the interior continuously slackened with the exhaustion of radioactive elements. Short-lived isotopes (^{26}Al, ^{36}Cl, ^{60}Fe, etc.) almost completely decayed during the first tens Ma of the Earth's life. The heat released thereby was added to the energetic effect of accretion. Giant bodies that reached the size of Mars participated in the accretion at its last stages. According to current concepts [80], the energy realized during accretion was sufficient to form an ocean of magma, i.e., an almost completely fused silicate shell, and to separate the Fe–Ni metallic core, which formed almost completely over a relatively short time span (~70 Ma) [80].

After formation of the Moon, the kinetic energy of the Earth's rotation, slowed down by tidal friction, was transformed into heat; however, this heat release yielded to other sources and diminished by an order of magnitude already over the first billion years of the Earth's life. The contemporary dissipation of tidal friction energy in different geospheres, i.e., internal friction within the solid Earth, can undoubtedly be neglected [77].

The observed "surface" HF (measured at a drilled depth interval, i.e., nearly at the boundary of solid Earth), whose density is $q_{sur} = -k\,\mathrm{grad}\,T$, differs from the deep HF because of effect of many distorting near-surface factors: morphology and contrast of thermal conductivity (k) of geological bodies, circulation of underground water, climatic temperature variation at the bottom of the heliothermozone, topography, tectonic movements, etc. Nevertheless, even for the small number of HF measurements available in the mid-20th century, it became evident that HF variations are related to regional physical and chemical processes [35]. When density of the surface HF is averaged over large regions, the opposite in sense effects of distorting factors are mutually compensated to a certain extent, so that average regional q_{sur} values are closer to deep HF than particular measurements.

Comparison of these values with the age (t) of tectonic and magmatic activity in large domains of the continental crust corresponding to fold regions differing in age reveals a significant correlation between these parameters, i.e., the HF–age dependence [21, 22, 37, 38, 45, 74, 82] (Fig. 1).

The q–t trend in the continental crust is especially striking in Phanerozoic blocks, where the HF structure consists of three components: (I) radiogenic heat produced in the crust; (II) time-dependent thermal perturbation related to tectonogenesis, or orogenic heat [82]; and (III) heat supply from the mantle. The latter is a result of decay of the still-retained radioactive ^{238}U, ^{232}Th, and ^{40}K isotopes, the manifestation of

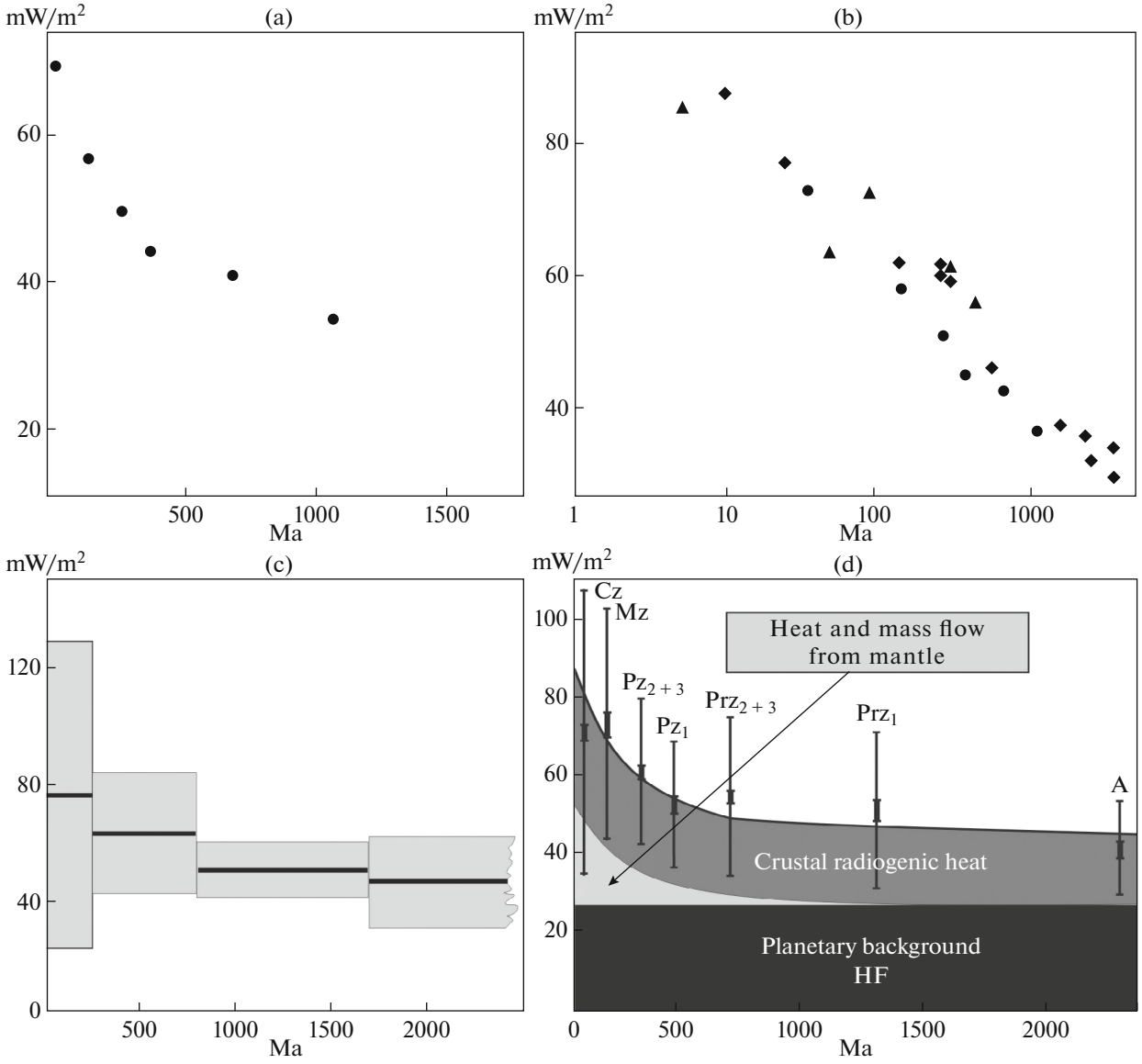

Fig. 1. Surface HF versus age of tectonomagmatic activity in continental crust: (a) after [22]; (b) circles after [22], diamonds after [13], triangles after [37]; (c) after [75, 76]; (d) after [82].

high-energy processes that occurred at the very early stages of the Earth's evolution, a certain contribution of gravigenic heat released by subduction of eclogitic and granulitic slabs into the mantle, and, probably, deep-seated exothermic geochemical processes.

When the number of measurements is increased, the dispersion of "synchronous" values of surface HF and q_{sur} observed in the same geoblock but at various spots or depth intervals also increases. This scattering obscures the general trend, so some skeptics doubt its existence [65]. These doubts have been dispelled, however, by four selections clustered by the isotopic age of rocks in the observation areas: <250, 250–800, 800–1700, and >1700 Ma [75, 76].

The Phanerozoic q–t trend makes it possible to identify component II by means of the traditional, for geophysics, solution to the inverse problem, i.e., by creating calculated thermal physical models, where the source depth, its shape, size, thickness, and time of existence are fit to variation of q_{sur} (see [14, 27, 30] and others). In such an approach, the geological nature of these temporal and local heat sources remains unknown, so that they are a priori identified with the upwelling of hot mantle material (asthenospheric diapirs). The validity of this postulate can be proved only by direct compositional evidence for invasion of the mantle material into the crust in zones with elevated HF.

This has been done owing to the study of He isotopes in subsurface fluids. As it turned out [15, 23], the

$^3He/^4He$ ratio (R) varies from ~10^{-8} in the subsurface water of Precambrian shields to ~10^{-5} in gases of volcanoes and hydrotherms of mobile belts and other objects genetically related to differentiation and degassing of the mantle. At the shields, this ratio corresponds to radiogenic helium, which appears owing to decay of U and Th contained therein at their global mean concentrations. In gases from active volcanism domains, the ratio is 1000 times higher because of the occurrence of primordial helium with $R \sim 10^{-4}$ entrapped by the Earth during accretion. In Phanerozoic folding zones, this ratio is intermediate in value and decreases with the age of tectonomagmatic activity and HF density. Thus, the latter positively correlates with relative concentration of ^3He rather than ^4He in terrestrial gases.

This implies that the ordered HF variations in the Phanerozoic tectonic provinces are related to mantle-derived heat and mass transfer rather than to crustal radiogenic heat. This heat and mass transfer has a silicate nature, as follows from the isotopic compositions of volatile helium and lithophile strontium in recent volcanic and hydrothermal activity products [24, 47, 48, 62].

Almost simultaneously with the revealed heat flow–age dependence, the relationship between surface HF (q_{sur}) and RHG (A_{sur}) has been found. The latter parameter reflects the total effect of decay of radioactive U, Th, and K isotopes in surficial, i.e., exposed or drilled, rocks [36, 53, 67]. Already after the first A_{sur} determination, it has become clear that RHG must decrease with depth. If this parameter remains constant throughout the crust, then surface HF would be at least by an order higher than the observed value.

The positive correlation of q_{sur} and A_{sur} has been established by comparison of pairs of these parameters in two of three studied regions of the United States [54, Figs. 3–9]. This relationship is described by the linear equation $q_{sur} = DA_{sur} + q_{red}$, where D is a coefficient numerically equal to $\tan\alpha$ (α is a slope of the regression line) with the linear dimension, because $\Delta q/\Delta A = |(W \times 10^{-3}\ m^{-2})/(W \times 10^{-6}\ m^{-3})|$, and determines in quantitative terms the thickness of the layer where heat generation is especially intense, i.e., the characteristic depth as defined in [73]; q_{red} corresponds to point $A_{sur} = 0$ (so-called reduced HF supplied to the sole of this layer). Parameter D characterizes the degree of differentiation of crustal matter by the content of radioactive elements. The parameter D is lower, the faster their concentration decreases with depth [50, 73].

Various models of radioactive element distribution, e.g., stepwise, linear, or exponential, can correspond to a decrease in RHG with depth. In the first model, the RHG value is taken as constant from the surface to depth D, and deeper jumpwise decreases up to the values inferred from the geophysical properties of corresponding layers. In the linear model [53], RHG decreases with depth according to the law $A_z = A_{sur}[1 - (z/(2D))]$; $0 < z < 2D$, where z is depth. In the exponential model [67], the decrease in RHG is described by the relationship $A_z = A_{sur}\exp(-z/D)$.

The concentration of each heat-producing radioactive element decreases with depth to a different extent. This differentiation is controlled by the processes occurring at various depths: primary separation into crust and mantle, magmatism, metamorphism, ascending advection of fluids, and circulation of meteoric underground water mainly in the supergene zone [50, 72].

The character of the vertical U, Th, and K distribution is clearly documented by boreholes in the Canadian Shield and the southern African Platform, e.g., in the Vredefort structure [60]. These data, which reflect different parameters D for each heat-generating element, make it possible to derive the reduced HF from the equation $q_{sur} = q_{red} + D^U A^U_{sur} + D^{Th} A^{Th}_{sur} + D^K A^K_{sur}$ [50], as well as the total RHG at different depth levels in the crust; however, the vertical features of A^U, A^{Th}, and A^K have been established only in a few cases.

After [59], the calculated q_{red} became identified as a mantle HF. The latter, however, is understood as ascending HF at the M discontinuity rather than at the D boundary, i.e., at the bottom of the crust (q_M), although q_{red} in principle differs from q_M, first, by the heat generation value in the middle and lower crust, second, owing to the lateral heterogeneity of the thermal conductivity existing there [43, 63], and finally, taking into account effect of "thick lithospheric mantle roots" on the HF [72, p. 396].

Setting the exponential model of the decreasing RHG with depth, we can determine the value of the crustal (radiogenic) contribution to surface HF (q_{cr}) by the integral

$$q_{cr} = \int_0^M A_{sur} D[1 - \exp(-M/D)],$$

where M is the crust thickness (Fig. 2). Thus, $q_M = q_{sur} - q_{cr}$. It was proposed to call regional selections differing in the value of parameter D *HF provinces* [36, 53, 67, 68] without specification of this flow. However, the q_{sur} and A_{sur} values in these provinces are characterized by a wide dispersion, which predetermines the possibility of its recognition, so that the traditional term—HF province—does not adequately express their specificity. The latter is much more evident in the constancy of the D and q_{red} values, which differ in particular regional selections. Therefore such $(q - A)_{sur}$ selections should be called by another term, e.g., D- or q_{red}-province, as proposed in [68]. As emphasized above (see also [59]), the reduced HF (q_{red}) differs little from the mantle HF, so that the D- or q_{red}-provinces could be called mantle HF provinces with that reservation. In some cases, they incorporate domains of tectonomagmatic activity differing in age,

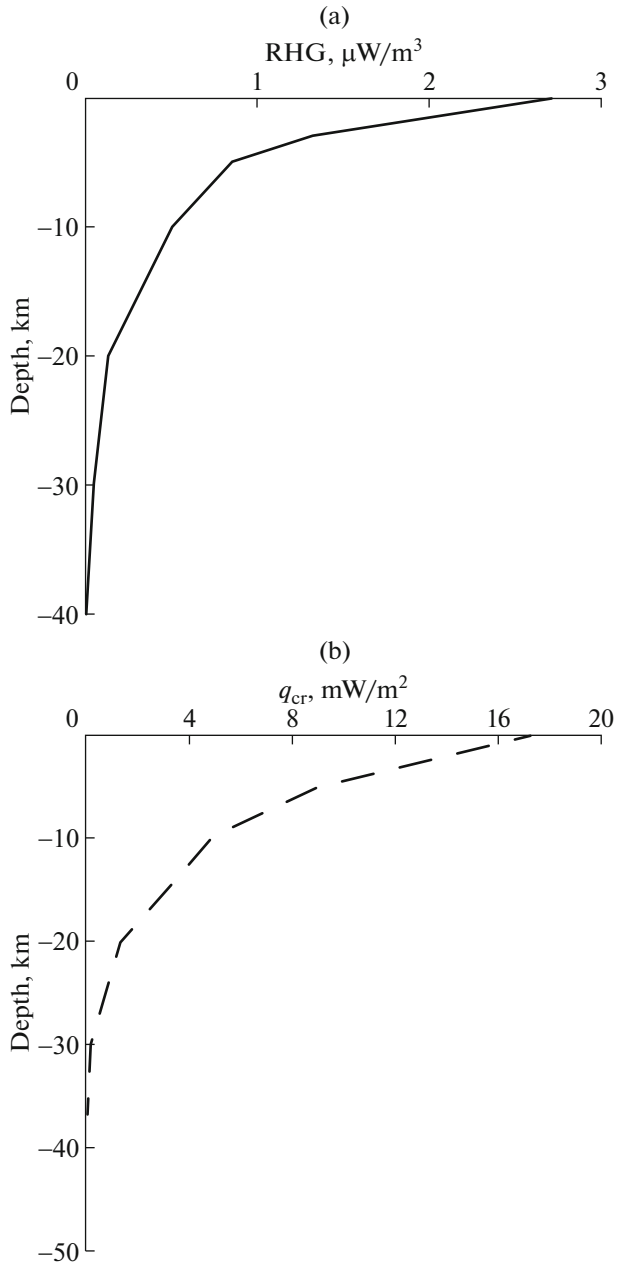

Fig. 2. Decrease of (a) RHG with depth according to exponential model at A_{sur} = 2.6 μW/m^3 and M = 50 km and (b) radiogenic crustal component of HF, q_{cr}.

where geothermal and He isotopic traces of heat and mass transfer is not yet relaxed, so that relationships of these domains and $(q - A)_{sur}$ provinces await further research.

RADIOGENIC HEAT FLOW IN GEOBLOCKS DIFFERING IN AGE

Archean–Proterozoic Geoblocks

The aforesaid shows that the HF structure, i.e., the proportion of its crustal and mantle components, remains incompletely clear. The most effective studies, which focused on the quantitative contributions of these components to HF, have been carried out on ancient platforms. Substantial data in this respect have been obtained from deep drilling in the Canadian Shield and South Africa [58, 64, 71, 72], as well as in the Baltic Shield (Kola Superdeep) [12].

The estimates of the crustal and mantle HF components in the oldest crustal blocks with known seismic structure are given in Table 1. It is assumed that in all indicated Archean and Proterozoic provinces, the crust thickness is 41 km, on average, and the mean density of the total surface HF (q_{sur}) is ~41 and ~55 mW/m^2 for the Archean and Proterozoic blocks, respectively.

These calculations are rather approximate, because in many cases, assumptions must be made from insufficient analytical data. For example, in Archean complexes 1, 3, and 4, the lower crust below 21 km, judging by the refractor velocity, is composed of granulites, for which RHG is estimated at 0.06 μW/m^3 [71] or 0.4 W/m^3 [63]. As a result, dispersion of the estimations of HF components reaches 20–25%.

As seen from Table 1, these components have been estimated more precisely for the Proterozoic blocks of Norway, owing not only to the data on HF and RHG in blocks of various middle and upper crustal rocks exhumed at the surface, but also to detailed gravity measurements. In northern Norway, where the crust the thickest (up to 43 km), its middle and lower parts consist of a 7-km sequence of amphibolites and granites, which overlie a 28-km-thick granulite sequence. The mean RHG = 2.2 μW/m^3 in this section ensures q_{cr} = 35 mW/m^2. In the Namaqua province of South Africa, where the mean heat generation is somewhat higher (2.3 μW/m^3), q_{cr} is estimated at ~40 mW/m^2. As follows from these data, the q_{cr} value varies from 20 to 45 mW/m^2, i.e., more than two times. This implies that this value hardly depends at all on the crust thickness and is controlled by surface heat generation and the rate of its decrease with depth, i.e., parameter D.

The RHG distribution was studied in the cover of the ancient East European Platform (EEP). N.S. Boganik carried out a detailed analysis of radiogenic heat generation in various crustal layers and lithotectonic zones of the platform [7]. According to these data, there are platform domains where the observed HF is completely provided by radiogenic heat generation, i.e., $q_{sur} = q_{cr}$ (Eastern Baltic Shield, Ukrainian Shield, Voronezh Crystalline Massif, western Pericaspian Basin). However, in most platform structures, the proportion of crustal and subcrustal HF has been determined as 9 : 1, and only at the platform's margin near the framing younger tectonic structures of the Carpathians, the Caucasus, and the Urals, does the share of heat supplied to the bottom of the crust reach 20% of the observed heat losses [7].

Table 1. Contributions of crustal and mantle components of HF in Archean and Proterozoic blocks of continental crust

No.	Complex (region, country)	Number of samples	A_{sur}, μW/m^3	D, km	HF, mW/m^2		Source
					crustal, q_{cr}	mantle, $q_M = q_{sur} - q_{cr}$	
	Archean						
1	Vredefort (SAR)	146	1.75	11	22–29	15–18	[60]
2	Lewisian (Scotland)	9	1.73	8.5	25–30	11–16	[83]
3	Kapuskasing (Ontario, Canada)	20	1.33	10.5	23–28	13–18	[34]
4	Pikwitonei (Manitoba, Canada)	–	–	–	20–23	18–21	[42]
5	Kirkland Lake (Superior, Canada)	64	1.08	14.4	23–26	14–18	[56]
6	Dharwar, India	2	1.05	7.5	22–25	12–16	[69]
	Proterozoic						
7	Northern Norway	23	2.31	8.4	34–35	18–20	[63]
8	Southern Norway	11	1.54	8.5	35	20–21	[78]
9	Catalina, (Arizona, USA)	155	1.13	15.5	>26–34	<21–29	[52]
10	Harkquahala, (Arizona, USA)	109	1.65	13	>32–44	<11–23	[52]
11	Aravalli (India)	4	1.6	14.8	35–38	28–31	[69]
12	Namaqua (SAR)	10	2.4	7.5?	39–43	13–18	[51]

Later, owing to more precise HF measurements in the EEP and to the improvement of the analytical basis of ^{238}U, ^{232}Th, and ^{40}K determination in core samples, the previous estimates were refined [13, 25, 26]. According to [26], 30–40% of the observed HF are supplied from the mantle in the Baltic Shield, Mesen Basin, Timan Ridge, and Pugachev Inlier and 40–45% in the Moscow Syneclise (boreholes near the towns of Danilov and Soligach). These estimates are comparable with the above data on other ancient geoblocks.

Unfortunately, the vertical variations of heat generation in the geological section of the EEP were not discussed. Based on the distribution of radioactive elements in carbonate and clay facies of the EEP cover (Fig. 3), it was concluded that this distribution in Archean, Proterozoic, and Phanerozoic rocks does not obey an exponential law and is mainly controlled by the lithology of rocks in large stratigraphic intervals [7].

Two reasons, as a minimum, apparently explain the lack of regular vertical heat generation distribution in the sedimentary cover of the EEP. First, this is the difference in provenances of the sedimentary material forming the cover. In the Early and Middle Paleozoic, the mountainous massifs in the territory of the present-day Baltic and Ukrainian shields were the main provenances [20]. Beginning from the Carboniferous, clastic material was supplied from the Urals and Timan, whereas in the Mesozoic, the Caucasus and Carpathians became provenances. It is hardly possible to expect any regularity in the vertical RHG distribution when such different sources of sedimentary material exist. This is supported by the diagram shown in Fig. 3. The second cause is formation of particular sedimentary complexes during different time spans and different duration of radiogenic isotope differentiation, if this process proceeded in the cover. No other matter transfer except for circulation of meteoric water was operated and is operating now.

Nevertheless RHG in the cover of EEP can be estimated on the basis of ^{238}U, ^{232}Th, and ^{40}K concentrations in the rock complexes [7]. The calculation has shown that radiogenic heat flow produced in the cover of EEP ensures only 3.7–5.0 mW/m^2 in the observed HF, whereas 20–22 mW/m^2 are generated in the plate basement [3, 26]. Thus, the total average RHG in the EEP is 24–27 mW/m^2, or 60% of the mean background HF, which is estimated at 42 mW/m^2 for EEP.

At the Siberian Platform, the RHG has been studied thoroughly in the Chara–Olekma Block of the Aldan Shield [19]. This shield is the largest inlier of the crystalline basement, which is overlain by a thin cover

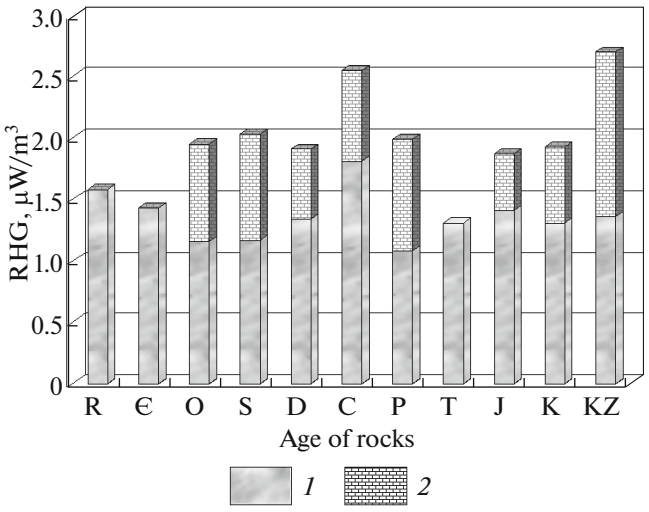

Fig. 3. Heat generation distribution in (*1*) clay and (*2*) carbonate facies of EEP cover, after [7].

of Upper Proterozoic and Phanerozoic sedimentary rocks only in the north and northeast and contacts with blocks subjected to Baikalian folding in the south and west.

The oldest basement rocks (infracomplexes) are represented by gneiss, crystalline schist, and charnockite dated back to 3 Ga. The U, Th, and K contents and, correspondingly, RHG in gneiss (1.25–2.14 μmW/m^3) and charnockite (0.66–1.28 μmW/m^3) vary widely owing to different structural levels of the Earth's crust, initial composition of protoliths, and apparently to the changeable grade of metamorphism and granitization within infracomplexes of the Chara–Olekma Block. The mean surface heat generation (A_{sur}), calculated in proportion to block areas (infracomplex inliers), is estimated at 1.09 ± 0.07 μmW/m^3 [19].

The younger supracomplexes are composed of metamorphic volcanic–sedimentary rocks diverse in composition: crystalline schist, quartzite, calc-silicate, and carbonate. Their relative amounts range within wide limits. A_{sur} in this part of geological section is 0.83 ± 0.11 μmW/m^3.

The upper structural stage of the basement is represented by thick Paleoproterozoic sequences of subplatform terrigenous and volcanic rocks. Large and compositionally heterogeneous massifs of plutonic rocks formed at the same time. Their heat generation is very variable. For example, A_{sur} in leucogranite is estimated at 0.56 to 3.99 μmW/m^3, while its mean value in rocks from the upper stage is 1.9 ± 0.9 μmW/m^3 [19], i.e., twice as high as in the underlying sequence.

Figure 4 compares the RHG in the Chara–Olekma Block with observed HF [4]; q_{sur} and A_{sur} show a significant positive correlation ($n = 9$; $r = 0.982 > 0.666 = r_{crit}^{0.05}$ approximated by the equation $q_{sur} = 18.5 + 13.5A_{sur}$. Setting the exponential model of heat generation distribution, the crustal HF has been calculated by integration within a depth interval from 0 to 40 km (M boundary). Integration yields 20.2 mW/m^2.

The surface HF in the Chara–Olekma Block varies from 30 to 48 mW/m^2, 38 ± 4.5 mW/m^2, on average. Subtracting the estimated value of crustal HF (20.2 mW/m^2), we obtain the value of the mantle component (~18 mW/m^2).

The proportions of crustal (radiogenic) and mantle components of HF in the Canadian Shield, EEP, and Aldan Shield show that the mantle HF for all objects approximately coincides; the ratio of both components is estimated at (55–60) : (45–40)% in favor of the radiogenic. Depth parameter D at the Aldan Shield is, however, three times greater than at the Canadian Shield and EEP. This is formal evidence of a less differentiated section in terms of concentrations of heat-generating elements. The complete lack of corresponding data makes it impossible to propose a more reliable model of their depth distribution.

Paleozoic Foldbelts

The description of the HF structure in the Paleozoides is based on detailed data mainly obtained at ore deposits of the Central Asian Foldbelt (CAFB), where the concentrations of radioactive elements have been determined in core samples with subsequent calculation of RHG. Typical data on other Paleozoic HF provinces are given in Table 2.

In these provinces, reduced HF amounts to 28–50% of surface HF (39.3 ± 10.3%, on average). The absolute value of the reduced (to a first approximation, mantle) flow in the Paleozoides is higher than in the Precambrian blocks; however, the crustal component of observed HF remains the same as in Archean and Proterozoic provinces. Two features of the Paleozoic geoblock attract attention as compared with older blocks: (1) higher values of parameter D indicating lower differentiation in younger blocks and (2) anomalously low q_{sur}, q_{red}, and D values in the southern Urals. The anomalously low values of observed HF in the northern Eurasia have also been noted in the northern Salairian Anticlinorium, the Gorlovsk Trough, the adjacent part of the Tom–Kolyvan Zone [29], and in the Hercynian South Mongolian Foldbelt [30, 31]. One of the reasons for this phenomenon is the decrease in its mantle component down to 4–5 mW/m^2, as observed in the Urals; however, it cannot be ruled out that there are several reasons for the anomalous reduction in both observed and mantle HFs [25, 29].

To explain this phenomenon, a model of mantle HF screening by allochthonous lithospheric sheets during the final stage of crust rearrangement in the Late Paleozoic Ocean has been proposed [30]. The mantle HF was consumed almost completely to heat the lower allochthon at a depth commensurable with

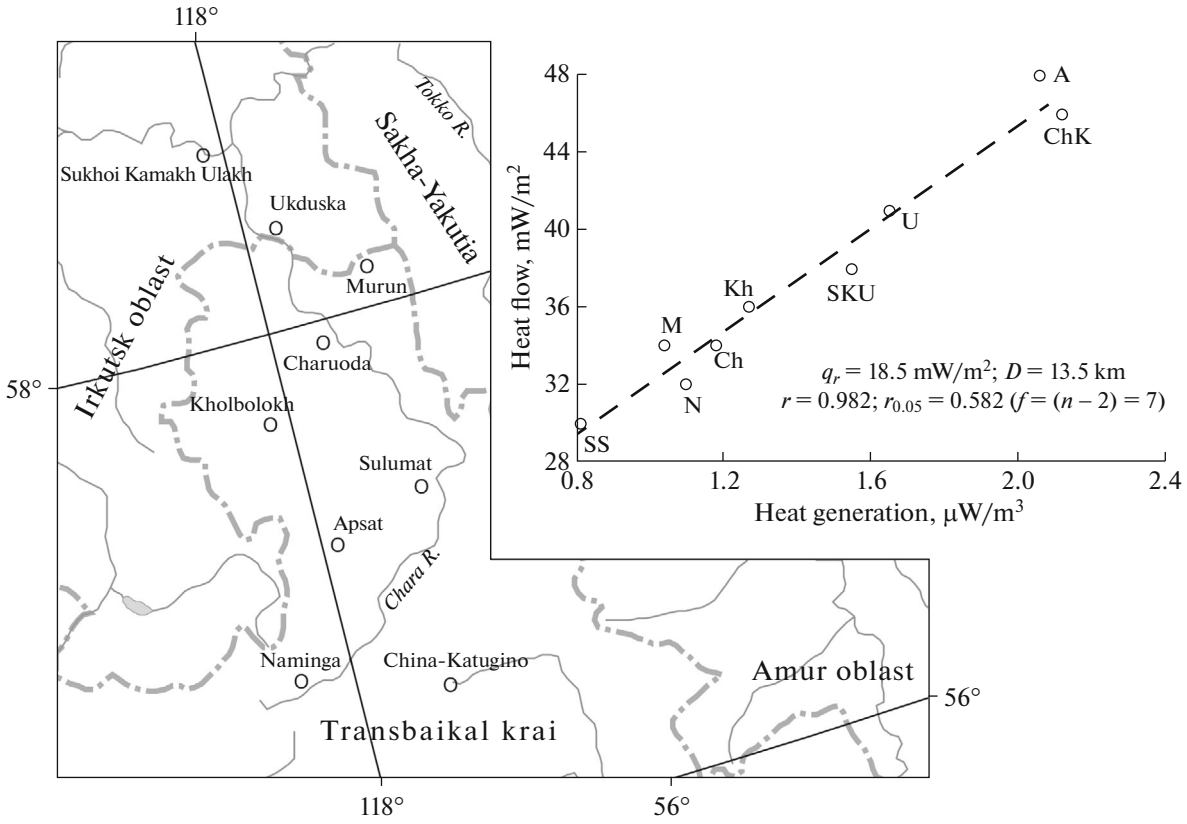

Fig. 4. Heat flow in boreholes of Aldan Shield after [14] versus surface heat generation in Chara–Olekma Block after [19]. Boreholes: M, Murun; SKU, Sukhoi Kamakh Ulakh; Ch, Charuoda; Kh, Kholbolokh; SS, South Sulumat; A, Apsat, U, Ukduska; N, Naminga; ChK, China-Katugino. See inset for borehole location.

the thickness of the oceanic lithosphere (70–80 km), i.e., much lower than M boundary. Calculation has shown that the time-dependent thermal regime that arose at those geometric screening parameters may continue for more than 300 Ma; i.e., it is felt in the contemporary thermal field.

Another reason for the lower HF in these regions could have been anomalously low concentrations of long-lived radioactive isotopes. However, the available data on the contents of radioactive isotopes in rocks of the Southern Urals and Salair do not exhibit a decrease in the ^{238}U, ^{232}Th, and ^{40}K concentrations [16], so that a smaller value of the mantle component is a more probable reason for the low observed HF in these regions.

The first estimates of heat generation (A) for the Kazakhstan territory of the CAFB have been obtained by calculations for separate lithospheric layers based on the mean content of heat-generating elements in each layer bounded by seismic surfaces with certain refractor velocities [6, 26] (Table 3).

The obtained RHG values for the given layered model of the CAFB can be approximated by an exponential decrease in heat generation with depth. If it is assumed that A_{sur} = 2.31 μW/m^3, then at the sole of the active heat generation layer A_D = 2.31 : 2.718 = 0.85 μW/m^3. In this case, the sole of layer D occurs approximately in the lower part of the granitic–metamorphic crustal layer. Interpolating the heat generation values for particular layers, we find that A_D = 0.85 μW/m^3. As follows from interpretation of the DSS data for the CAFB, e.g., along the Balkhash–Temirtau, Temirtau–Petropavlovsk, and Temirtau–Samara seismic lines, the total thickness of the granitic–metamorphic crustal layer is estimated at 15–16 km [Yu.K. Shchukin, personal communication 1992], and its lower part with refractor seismic velocities of 5.7–6.3 km/s is located within the depth interval of 11–16 km. Thus, based on the layered (stepwise) model of decreasing surface heat generation, we suggest that D ~ 13.0–13.5 km.

Let us verify whether the depth of the active heat generation layer (D) is located in this depth interval, when the exponential model of decreasing heat generation is used.

Constructing this model for each borehole, where HF is measured, we calculate A_{sur} from formula

$$A_{sur}\ (\mu W/m^3) = 0.132\rho(0.718U + 0.193Th + 0.262K),$$

where U, Th are the uranium and thorium concentrations, ppm; K, wt %, and ρ is the rock density, g/cm^3.

Table 2. Parameters of Paleozoic HF provinces

Province	Age, Ma	HF, mW/m^2	Radiogenic HF, mW/m^2	Reduced HF, mW/m^2	Parameter D, km	Th/U	Source
Appalachians and New England (USA)	400–100	47 ± 17	24 ± 18	23 ± 4	7.5 ± 0.2	4.2 ± 1.1	[68]
England and Wales	600–300	59 ± 23	34 ± 23	25 ± 3	16 ± 1.6	1.5	[55, 66]
Norway	450–250	50 ± 15	30 ± 15	20	8.4	3.3 ± 1.5	[78]
Iberian Meseta	350–250	46 ± 12	34 ± 12	13	11.5	3.5	[32]
Altai, Sayan, West Siberian Plate	600–250	52 ± 22	35 ± 23	17 ± 8	16 ± 1.8	4.6	[29]
Tien Shan	450–250	56 ± 16	33 ± 17	22–25	12.5	5.1 ± 1.3	[18, 30]
South Urals	400–320	32 ± 6	27 ± 7	5 ± 4	6.6 ± 2.3	6.3 ± 2.5	[25, 30]

Table 3. Heat generation in lithospheric layers

Lithospheric layer	Heat generation (A), μW/m^3	Refractor seismic velocity (v_r), km/s
Granitic–metamorphic	1.55	5.1–6.3
upper part	2.31	5.1–5.7
lower part	1.26	5.7–6.3
Basaltic	0.46	6.3–8.3
upper part	0.67	6.3–7.3
lower part	0.25	7.3–8.3
Upper mantle	0.008	8.3–8.4

The empirical data obtained in Borehole 503 at the Bestyube deposit show that the RHG distribution along the depth can be approximated by the exponential model (Fig. 5). The smoothing exponential curve is constructed with aid of STATISTICA program. The obtained RHG distribution is described by the equation $A_z = 1.2\exp(z/12)$ at $r^2 = 0.591$ ($r_{0.05} = 0.497$) for the bilateral Pearson criterion. In the above formula, A_{sur} is 1.2 μW/m^3 for the Bestyube deposit, and value of 12 km in the denominator of exponent is parameter D for the same structure. The D estimates for the layered and exponential models of decreasing RHG for the Bestyube deposit are close to each other. Now we pass to subsequent analysis of the heat generation parameters for the entire set of data on the CAFB.

The relationship of HF measured at ore deposits of Kazakhsatn, the Tien Shan, and Mongolia versus surface heat generation (A_{sur}) is shown in Fig. 6. As is seen from this figure, the observed HF varies from 20 mW/m^2 at the Tavan-Tolgoit coal field in the South Mongolian Foldbelt to 94 mW/m^2 at the Uchkoshkon tin deposit in the Kokshaal Zone of the South Tien Shan. The interval of A_{sur} from 0.44 μW/m^3 at the same Tavan-Tolgoit to 3.9 μW/m^3 at the Aktogai porphyry copper deposit in the Balkhash Basin is no less significant. (Data on radioisotope concentrations in the Borly, Karkaralinsk, and Aktau-Mointy boreholes were kindly placed at our disposal by A.M. Kurchavov from the Institute of Geology of Ore Deposits, Petrography, Mineralogy, and Geochemistry, Russian Academy of Sciences and are published with his permission.) This data set shows a linear correlation: $r = 0.555$ ($r_{0.05} = 0.323$ for $n - 2 = 27$). The dependence of HF vs. RHG is approximated by the equation $q_{sur} = 24.7 + 13.3A_{sur}$.

As is seen from Fig. 6, q_{red} is 24.7 mW/m^2 and D = 13.3 km. These values almost coincide with estimates for the Bestyube deposit and for the results of calculations using stepwise model for the Kazakhstan territory of CAFB. All they indicate that sole of the active heat-generating layer occurs in the lower part of the granitic–metamorphic layer.

Opening the integral approximation for calculation of the crustal HF (see above), we obtain the formula $q_{cr} = DA_{sur}[1 - \exp(-M/D)]$.

After substitution of the corresponding parameter values for the CAFB areas into this formula, we obtain the calculated value of crustal (radiogenic) HF (27.2 mW/m^2). Taking into account the uncertainties of our estimates, we see that ratio of crustal (radiogenic) to mantle HF is 50 : 50%.

Areas with Anomalous Radiogenic Heat Generation

An anomalously high RHG has been revealed for Permian magmatic bodies in two areas of the Eurasian continent. These are the Akchatau biotite granite pluton in the Tokrau Basin of central Kazakhstan [30] and the tin-bearing Carnmenellis granitic pluton in the Cornwall Peninsula in southwestern England [84]. Let us consider the HF structure of these areas in more detail.

Akchatau pluton

The highest HF density in central Kazakhstan (q_{sur} = 77–78 mW/m^2) has been measured at two sites of the Akchatau pluton. This rare-metal deposit is related to the conjugation zone of the Shetsk Anticlinorium with the Tokrau and Akzhal–Aksoran synclinoriums subjected to complex folding and faulting and cut through by granitic plutons of the Middle–Late Carboniferous Topar intrusive complex and Late Permian–Early Triassic Akchatau complex. The coarse-grained leucogranite of the Akchatau Complex, which hosts the deposit, forms a massif consisting of three consecutively emplaced intrusions [10].

The total thickness (10 km) of the Akchatau intrusive complex was estimated along the Balkhash–Temirtau DSS profile. This increases the thickness of the granitic–metamorphic layer as a whole. Its upper zone is limited to the refracting surface with v = 5.7 km/s at a depth of 10 km, while the lower zone limited by the surface with v = 6.3 km/s at a depth of 20–21 km. The total crust thickness also increases to 44–47 km, whereas to the north and south, the crust is thinner (39–40 km) [1].

The geothermal research at the Akchatau deposit included thermometric measurements in eight boreholes and collection of core samples to determine heat conductivity and U, Th, K contents. The geothermal gradient at the Akchatau varies from 21.6 to 26.0 mK/m (Fig. 7). These are the highest values among all other determinations made in the Central Kazakhstan mosaic fold region [30].

Three rock complexes are distinguished by heat conductivity (k): felsic lava and tuffs with k = 2.57 ± 0.08 W/(m K); biotite granite (2.97 ± 0.07 W/(m K)), and greisen (4.09 ± 0.42 W/(m K)).

With allowance for corrections to refraction of the HF under conditions of contrasting heat conductivity, its surface density (q_{sur}) has been determined. At two sites differing in orebody morphology, q_{sur} varies from 68–72 mW/m^2 (Northern site) to 71–78 mW/m^2 (Aksai site) [30]. To explain the nature of such a high conductive HF, we quantified its crustal and mantle components, taking into account the contents of heat-generating isotopes in the rocks penetrated by boreholes. The results are given in Table 4.

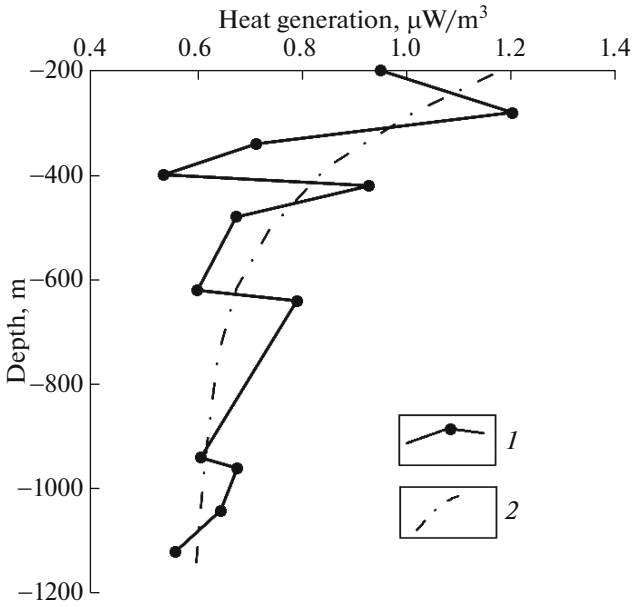

Fig. 5. Heat generation versus depth in Borehole 503 at Bestyube deposit. (*1*) Empirical heat generation value; (*2*) exponential smoothing curve of heat generation distribution.

The rocks in sections of the aforementioned sites of the deposit are characterized by an extremely high RHG, which exceeds by four to five times the heat generation in the granitic–metamorphic layer of the Late Paleozoic Dzhungar–Balkhash Fold Region [26]. The especially high RHG values are established in the upper part of the contact zone of the ore with host rocks. Such anomalously high heat generation is an obvious attribute of the Akchatau intrusive complex being composed of leucogranites. Therefore, the thickness of the pluton should be taken into consideration when the crustal and mantle components of HF are calculated. Thus, we have estimated HF components, issuing from stepwise and exponential models of RHG distribution.

Applying the stepwise model of RHG distribution, its values in the lower part of granitic–metamorphic and in the basaltic layers have been taken from the literature [26]. According to this model, the crustal HF is 40 mW/m^2. The remainder of the measured HF (30–35 mW/m^2) characterizes the heat removal from the mantle.

The calculation by exponential model requires estimation of parameter D, which has been calculated using the technique described above and yielded 3.8 km. After substitution of the obtained D value into equation $q_{cr} = DA_{sur}[1 - \exp(-M/D)]$, the crustal HF have been assessed as 37.5 mW/m^2 in agreement with the above calculation based on the stepwise model. Accordingly, in the exponential model, the reduced HF is 32–37 mW/m^2.

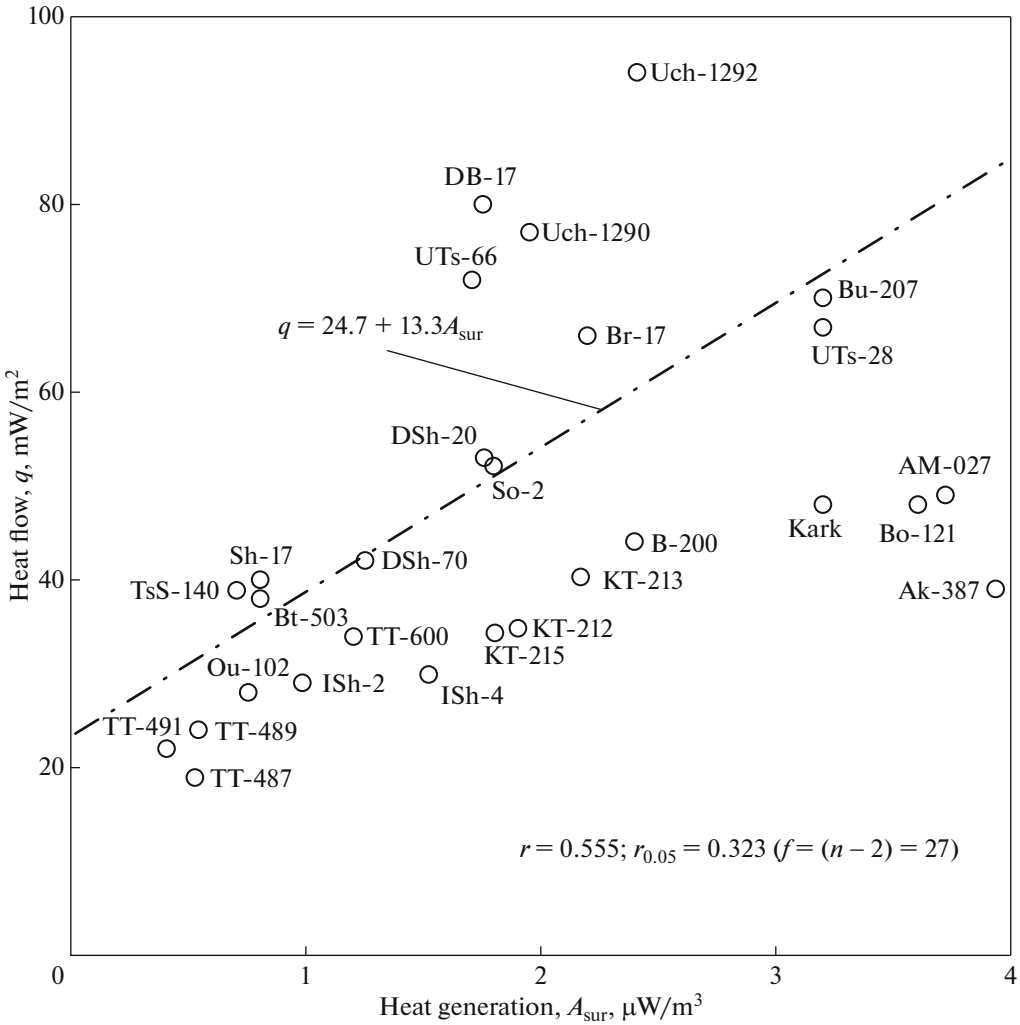

Fig. 6. Heat flow (q) versus surface heat generation (A_{sur}) at ore deposits of CAFB. Symbols represent deposit names and borehole numbers: Uch, Uchkoshkon (South Tien Shan); DB, Dund-Bulag; UTs, Ungur-Tsagan; Br, Berkh; Bu, Burinkhan; DSh, Dzan-Shire; Sh, Shand; TsS, Tsgan-Suburga; TT, Tavan-Tolgoyt; Ou, Ouyut; Ish, Ikh-Shanhai (Mongolia); Bt, Bestyube; So, Saryoy; Bo, Borly; KT, North Katpar; Ak, Akbokay; Kark, Karkaralinsk; AM, Aktau–Mointy (central Kazakhstan).

In discussing the exponential simulation results, it should be emphasized once again that the reduced HF corresponds to the mantle HF incompletely. The point is that granite of the Akchatau pluton also occurs beneath the layer of active heat generation, i.e., deeper than 3.8 km, and it is unreasonable to ignore the occurrence of radioactive isotopes therein. Though their concentrations are three times lower than in the upper 4 km, they nevertheless ensure the heat generation measured by 2–4 μW/m^3. These values are by an order of magnitude higher than in the mantle. Extrapolating the decrease of heat generation with depth along the exponent to the M boundary and calculating radiogenic HF in the lower crust, we obtain 5.5 mW/m^2. Thus, the exponential model of heat generation distribution yields a more reliable value of HF from the mantle (26.5–31.5 mW/m^2). This value is 2–5 mW/m^2 higher than estimates of the mantle HF in other areas of the CAFB.

It is evident that the high radiogenic crustal HF in the Akchatau pluton is caused by high concentrations of ^{238}U and ^{232}Th [5, 50]; however, the nature of HF from the mantle exceeding its estimates in other Late Paleozoic structures of CAFB requires further discussion and refinement.

This elevated mantle HF may be evidence that the zone of fractional melting of the mantle matter (the astenosphere roof) approaches to the Earth's surface. According to our estimates, the thickness of the lithosphere beneath the Tokrau Basin is 130–140 km, whereas beneath the adjacent structures of central Kazakhstan it is appreciably greater: 370 km in the Selety Synclinorium, 330 km in the Uspensky Zone, and 170 km near Lake Balkhash [30]. In turn, the

decrease in thickness of the lithosphere can be related to younger tectonic activation of the structure. In addition to the Akchatau pluton of Early Triassic age that is younger in comparation with the ambient Late Paleozoic complexes [2] , the later (Mesozoic?) supply of mantle matter to the crust is supposed.

Carnmenellis Pluton

This is one of the merging granitic massifs that made up the large Early Permian (300–275 Ma) Cornubian Batholith that underlies the Cornwall Peninsula in southwestern England. The batholith is composed of tin granites that formed as products of partial melting of the sedimentary protolith. In the 1970s–1980s, some of its massifs were explored using physical methods, including thermics, and drilled to a depth of 2300 m [44, 46, 57, 79, 84, 85].

As was established by studying the Carnmenellis pluton, the accessory minerals from granite (monazite, zircon, xenotime, apatite, uraninite) contain radionuclides, which ensure heat generation in an amount of no less than 4 $\mu W/m^3$, which remains practically unchanged in the two upper kilometers of section [84]. This RHG is approximately two times more intense than the average of the granitic–metamorphic layer in the Earth's crust. The high RHG could have resulted in the observed conductive HF. Its density in the Carnmenellis pluton varies from 106 to 129 mW/m^2 [44]. This is much higher than the mean $q_{sur} = 55$ mW/m^2 in Great Britain [85]. As was pointed out above, the localization of the HF anomaly agrees closely with the morphology of the Carnmenellis pluton [55]. This anomaly should be attributed, however, not only to high local RHG but also to water circulation in the upper 2–3 km of the geological section [44] (Table 5).

To quantify the HF components, an exponential model of RHG diminution with depth has been adopted. Using the technique described above, the radiogenic component is estimated at 29 mW/m^2 and parameter D is 7.0 km. The thickness of the Cornwall batholites is ~15 km [85], so that the same situation develops here as in the Akchatau batholith, i.e., reduced HF ($q_{red} = 110 - 29 = 81$ mW/m^2), reflecting heat supply not only from the mantle, but also from the lower crust about 7 km above M boundary. The lower crust consists of metasedimentary rocks with interlayers of volcanogenic material and sporadic mafic intrusions. The contribution of the lower crust to the heat budget, if its nature is thought to be only radiogenic, is ~50 mW/m^2. In this case, the mantle HF is estimated at $81 - 50 = 31$ mW/m^2. This value is random but coincides with the estimate of mantle HF at Akchatau.

Importance should hardly be attached to this coincidence, because vertical fluid filtration, which is inferred within Cornwall plutons [44], distorts conductive HF by 7–8 mW/m^2 (Table 5). No evidence for the development of such filtration is known for the Akchatau pluton. On the contrary, the thermograms of boreholes (Fig. 7) are linear with small deviations caused by structural and thermal physical heterogeneities of the section.

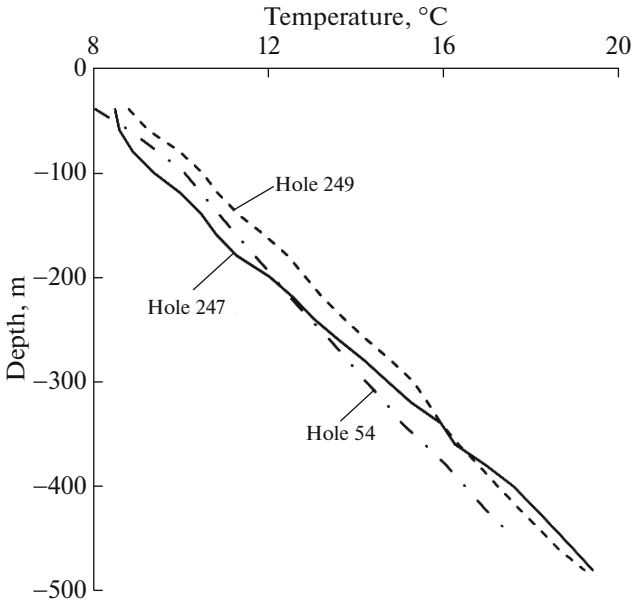

Fig. 7. Thermograms of boreholes at Akchatau deposit.

In the two examples above, the elevated concentrations of radioactive elements are sources of elevated HF in the crust. The cause of increasing HF below depth D (the layer of active heat generation) could be related to approach of mantle zone of fractional melting as a result of active tectonics, as was noted for Akchatau, or to intensified convection in the fracture system, as was proved for the Cornwall batholites.

In comparison with the aforementioned regions with anomalous RHG, even the contemporary Baikal Rift Zone (BRZ) with high background HFs (20–470 mW/m^2), 78 and 60 mW/m^2, on average for the lake and coast, respectively) is characterized by relatively modest radiogenic HF (up to 20–30 mW/m^2). The rest of the flow, 50–60 and 30–40 mW/m^2, is thought to be related to additional crustal and mantle heat sources [8]: mantle intrusions and intense hydrothermal heat and mass transfer. The effects of these sources are the most appreciable in rift basins, which are the most permeable in this region. Thus, the ratio of crustal to mantle HF in the BRZ is 30 : 70%.

DISCUSSION

The data considered above demonstrate an increase in mantle HF with rejuvenation of tectonic structures. It was assumed that the mantle component of HF varies in time from its maximum in the regions of contemporary active tectogenesis to the minimum or even almost

Table 4. Radiogenic heat generation at Akchatau deposit

Hole number	Depth, m	Content			RHG, μW/m^3
		U, g/t	Th, g/t	K, %	
Northern site					
38	80	9.5	41.5	4.3	5.8
	160	11.0	49.0	4.6	6.8
	200	69.0	32.9	4.4	20.8
	280	15.0	48.6	4.3	7.8
	300	28.0	57.4	4.3	11.8
43	80	50.0	41.0	4.0	16.4
	120	47.0	49.0	4.2	15.6
	214	10.6	27.5	3.4	5.1
97	60	9.5	52.8	3.4	6.6
	143	9.0	53.5	3.8	6.6
Aksai site					
249	40	5.1	18.3	4.2	2.9
	80	3.2	5.5	3.4	1.6
	240	9.6	15.5	3.5	4.2
	340	6.7	43.7	4.0	5.3
	360	34.0	42.5	3.4	12.2
	380	23.4	50.8	4.3	10.1
	460	7.5	49.5	4.0	5.9
	480	9.4	45.9	4.3	6.1
247	340	43.0	50.5	4.0	15.2
	375	14.9	45.2	4.2	7.5
	380	30.0	44.2	4.2	9.8

Table 5. Heat flow and heat generation in granitic plutons and basement rocks of Great Britain

Object	Number of HF measurements	q_{sur}, mW/m^2, average ± σ	HF corrected with allowance for one-dimensional model of fluid circulation, mW/m^2	RHG, μW/m^3
Cornwall plutons				
Carnmenellis	10	115 ± 7	108	4.0 ± 0.5
Bodmin	5	116 ± 5	109	4.2 ± 0.9
Lands End	3	125 ± 3	118	5.1 ± 0.2
Saint Austell	2	126 ± 0.5	118	4.2 ± 0.9
Dartmoor	6	113 ± 9	113	5.3 ± 0.5
Average	26	116.7 ± 5.2	113 ± 4.7	4.6 ± 0.5
Plutons of northern England	4	84.0 ± 14.2	–	4.1 ± 0.8
Plutons of Scotland	5	67.6 ± 13.5	–	5.5 ± 2.5
Basement rocks of central England and Wales	6	49.3 ± 10.4	–	1.4 ± 0.6

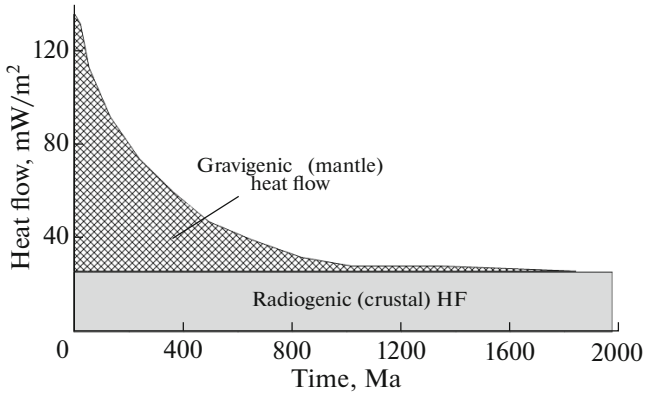

Fig. 8. Crustal and mantle HFs versus geological time under assumption that radiogenic HF is invariant throughout geological history.

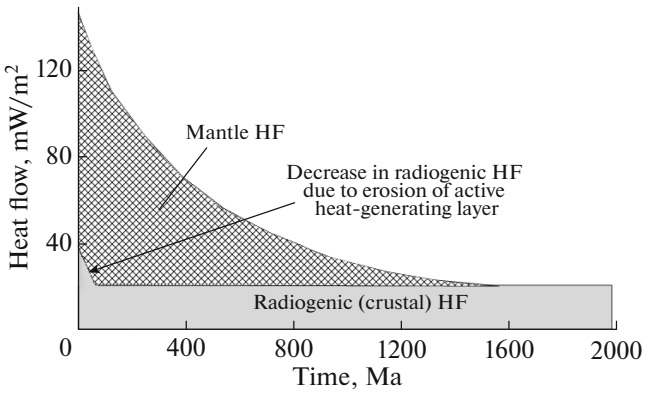

Fig. 9. Crustal and mantle HFs versus geological time with allowance for influence of upper RHG erosion.

zero in the Precambrian crust [13, 28, 40]. Crustal radiogenic HF serves as an time-invariant addition, the percentage of which relative to the mantle HF increases with time and, correspondingly, with a decrease in the mantle component (Fig. 8).

Another relationship between crustal and mantle HF has been proposed [82]: a twofold decrease in crustal (radiogenic) HF over 300–400 Ma due to erosion of the upper crustal layer enriched in radioelements (active generating layer).

But how much does erosion influence the amount of radiogenic heat released from this layer? This problem can be considered by the example of the CAFB and certain other Phanerozoic foldbelts.

According to Dobretsov [17], two parallel near-latitudinal zones of metamorphic rocks conformable to tectonic structures are recognized in the CAFB. The northern zone consists mainly of medium–temperature metamorphic rocks of epidote–amphibolite facies, whereas the southern zone is represented by low-temperature greenschist and glaucophane-schist facies. The latter, as is known, forms under conditions of low temperature (100–250°C) and relatively high pressure (6–12 kbar) [81]. The typical areas where this facies occurs are oceanic plate subduction zones [9]. They are noted in both active (Japan, Sakhalin, Kamchatka, California) and older Benioff zones (Penninian Alps, Sanbagawa Belt in Japan, Tien Shan, the Urals, eastern Kazakhstan, etc.). These are regions of low-temperature regime in the lithosphere controlled by plunging of relatively cold blocks. At the same time, this process is accompanied by stresses corresponding to the lithostatic load of the 40- to 45-km layer of the lithosphere.

Thus, the thermodynamic conditions of the subduction and obduction zones ensure development of glaucophane-schist and greenschist metamorphic facies. As was convincingly shown in [11], the South Mongolian Hercynian Belt, where these facies are widespread, formed as a result of subduction of the Paleotethian oceanic plate.

At the moment of closure of the Paleotethys in southern Mongolia 320–270 Ma ago, the temperature of glaucophane schist formation was achieved at a depth of 6.5–8.0 km [30], whereas at present these rocks crop out at the surface [17]. This implies that in the course of geological history, the upper 8 km of the crust have been eroded. Under the assumption that erosion developed at a constant rate over the entire post-Permian history, this rate was 0.03 mm/yr.

The northern Late Paleozoic metamorphic zone of the CAFB was characterized by the thermodynamic regime of epidote–amphibolite facies. According to our simulation, the temperature at a depth of 25–30 km was 450–500°C [31]. Similar reasoning leads to the conclusion that over 200 Ma after the formation of the arch in the northern Mongolian Megablock, 25 km of the crust have been eroded; i.e., its erosion rate is 0.12 mm/yr.

The calculated values of the erosion rate are relatively low in both cases. They are not much higher in other foldbelts; e.g., it is 0.8 mm/yr in the Alps [39] and 0.6 mm/yr in Scandinavia [70] and Scotland [41]. At such an erosion rate, a 10-km layer of active heat generation existing in the geological past could have been eroded over ~20 Ma.

Thus, in all Paleozoic and, moreover, Precambrian foldbelts, the surface RHG and, correspondingly, radiogenic crustal HF were much higher during their formation than the contemporary values. Peneplanation of foldbelts developed relatively fast as compared with their age. Therefore, it can be assumed that during the Archean, Proterozoic, and most of the Phanerozoic, the RHG did not change (Fig. 8). However, in the Mesozoic, and especially in the Cenozoic, erosion played a large role in RHG formation and diminished radiogenic HF (Fig. 9). As seen from this figure, the temporal trend of HF components is in principle similar to the dependence of HF on the age

of tectogeneis [82], but differs in the time scale of the erosion effect.

CONCLUSIONS

Summing up, it can be stated that two HF components are distinguished in the thermal regime of the lithosphere: the HF formed due to decay of radioactive elements in the Earth's crust and the HF supplied to its bottom from below (commonly called mantle flow). The origin of the latter is more complex. It is formed due to the effect of many stationary and time-dependent factors. In addition to radiogenic heat generation at subcrustal depths, these are transformation of the potential energy into heat during gravitational differentiation of the Earth's matter, residual heat of the planet accretion, the thermal effect of the Earth's rotation, and mass and heat transfer related to movement of subcrustal masses. The interaction of many factors controls the evolution of the mantle HF in geological time. The gradually waning intensity of geodynamic phenomena is a cause of the observed HF trend.

Due to the heterogeneous origin, it is almost impossible to calculate regional values of mantle HF directly. Therefore, these values are found as the difference between the total observed (measured) HF and radiogenic crustal HF. The latter is calculated using analytical data on U, Th, and K contents, which make the main contribution to the geoenergetic balance at the recent stage of the Earth's evolution.

Our estimates of the radiogenic component in crustal HF of the Archean, Proterozoic, and Paleozoic structures show that the difference between them is statistically insignificant; i.e., the crustal radiogenic HF remains invariant over an enormous time interval from 2000 to 250 Ma.

Exclusions are related to exotic geological situations. For example, biotite granites in the Akchatau and Carnmenellis plutons are enriched in radioactive isotopes to such a high degree that they produce radiogenic HF at least two times higher than the ambient background.

The radiogenic heat generation diminishes with depth. The maximum values are observed near the Earth's surface and become several times lower already at a depth of 3–5 km. The decrease can be approximated by various models. The model of exponential decrease in surface heat generation (A_{sur}) most adequately reflects the real pattern of depletion in radioactive elements in the Earth's crust. When surface heat generation and the thickness of the active heat-generating layer D are known, one can readily calculate HF in the crust by integrating the exponential function within the depth interval from the surface to the bottom of the crust.

The upper active heat-generating layer is destroyed by erosion, and this inevitably results in a decrease in surface heat generation and total crustal HF. However, the erosion rate and duration of peneplanation show that material is removed from the surface rather rapidly, so that the effect of erosion can be neglected when calculating radiogenic heat generation in the Paleozoic and, moreover, Precambrian foldbelts, because their age exceeds the characteristic time of topography planation by one to two orders of magnitude.

The ratio of the crustal and mantle components in the total observed HF varies depending on the time of the last tectonomagmatic activation. For Archean and Proterozoic structural units this ratio varies from 70 : 30 to 60 : 40% in favor of crustal radiogenic HF, whereas in Paleozoic crustal blocks, it is 50 : 50%. In the Cenozoic Baikal Rift Zone, this ratio is 30 : 70% with appreciable predominance of the mantle component.

Thus, the dependence of HF on tectonic age is caused by a decrease in heat supply from the mantle to the crust.

ACKNOWLEDGMENTS

This study is supported by the Russian Foundation for Basic Research (project nos. 14-05-00012 and 14-05-00082) and the Presidium of the Russian Academy of Sciences (program no. 4, project 2.8).

The authors discussed problems relevant to this paper with I.N. Tolstikhin (Geological Institute, Kola Science Center, Russian Academy of Science), who made important critical remarks. We thank S.M. Lyapunov and E.P. Shevchenko (Chemical Analytical Laboratory, Geological Institute, RAS) for determination of long-lived radioactive isotopes in rocks. We are also grateful to A.M. Kurchavov (Institute of Geology of Ore Deposits, Petrography, Mineralogy, and Geochemistry, RAS) for his data on U, Th, and K contents in rocks of central Kazakstan kindly placed at our disposal and to E.N. Aleksandrova for her assistance in the graphic design of the paper.

REFERENCES

1. A. P. Andreev, V. V. Brodovoi, and V. I. Gol'dshmidt, "Deep structure of the Earth's crust of Kazakhstan and technique of its study," Izv. Akad. Nauk Kaz. SSR, Ser. Geol., No. 4, 3–15 (1964).
2. R. M. Antonyuk, G. F. Lyapichev, N. G. Markova, T. G. Pavlova, O. M. Rozen, S. G. Samygin, S. G. Tokmacheva, V. I. Shuzhanov, and I. G. Shcherba, "Structures and evolution the Earth's crust of Central Kazakhstan," Geotektonika, No. **5**, 71–82 (1977).
3. N. I. Arshavskaya, "On lineiar dependence between heat flow and heat generation in shields," in *Eksperimental'noe i teoreticheskoe izuchenie teplovykh potokov* (Nauka, Moscow, 1979), pp. 177–194.
4. V. T. Balobaev, *Geothermics of the Cryozone within the Lithosphere of North Asia* (Nauka, Novosibirsk, 1991) [in Russian].

5. V. G. Bogolepov, N. A. Gulyaeva, and D. A. Safin, "On the technique of searching for ore bodies at Akchatau rare-metal deposit, Central Kazakhstan," in *Mineralogiya i geokhimiya vol'framovykh mestorozhdenii* (Nauka, Leningrad, 1975), pp. 55–65.
6. G. M. Baranov, A. A. Smyslov, and M. G. Kharlamov, "Radioactive elements content in intrusive rocks of the Selety-Korzhunkol' area, Central Kazakhstan," in Vol. 95 of *Tr. VSEGEI, Nov. Ser.* (1963), pp. 61–69.
7. N. S. Boganik, *Radiogenic Heat of the Earth's Crust in the East European Craton and Its Folded Framing* (Nauka, Moscow, 1975) [in Russian].
8. V. A. Golubev, S. V. Lysak, and R. P. Dorofeeva, "Teplovoi potok Baikal'skoi riftovoi zony," in *Teplovoe pole nedr Sibiri* (Nauka, Novosibirsk, 1987), pp. 121–137.
9. N. L. Dobretsov, V. G. Melamed, and V. N. Sharapov, "Dynamics of regional metamorphism for the model of simple immersion of the oceanic crust," Geol. Geofiz., No. 10, 16–24 (1970).
10. O. S. Klyuev, "Geochemical search for hidden mineralization: A case study of the Akchatau greisen deposit Central Kazakhstan," in *Geokhimicheskie metody prognozirovaniya i poiskov rudnykh mestorozhdenii* (IMGRE-ONTI, Moscow, 1976), pp. 32–53.
11. V. I. Kovalenko, A. A. Mossakovskii, and V. V. Yarmolyuk, "The problem of reconstructing the geodynamical settings and petrochemical zonality: A case study of the Mongolian Late Paleozoic volcanic belt," Geotektonika, No. 6, 13–29 (1983).
12. A. A. Kremenetskii, L. N. Ovchinnikov, and S. Yu. Milanovskii, "Geothermal studies and the heat generation model for the Precambrian crust of northeastern Baltic Shield," in *Geokhimiya glubinnykh porod* (Nauka, Moscow, 1986), pp. 131–149.
13. R. I. Kutas, *Heat Flow Field Pole and Thermal Model of the Earth's Crust* (Nauk. Dumka, Kiev, 1978) [in Russian].
14. R. I. Kutas and V. V. Gordienko, "Teplovoe pole Karpat i nekotorye voprosy geotermii," in Vol. 46 of *Tr. Mosk. O-va Ispyt. Prir., Otd. Geol.* (Nauka, Moscow, 1972), pp. 75–80.
15. B. A. Mamyrin, and I. N. Tolstikhin, *Helium Isotopes in Nature* (Energoizdat, Moscow, 1981) [in Russian].
16. G. A. Mashkovtsev, A. K. Konstantinov, A. K. Miguta, M. V. Shumilin, and V. N. Shchetochkin, *Uranium of the Russian Interiors* (VIMS, Moscow, 2010) [in Russian].
17. *Metamorphic Complexes of Asia*, Ed. by V. S. Sobolev (Nauka, Novosibirsk, 1977) [in Russian].
18. E. L. Mozoleva, "Heat generation of rocks in Tien Shan," in *Geotermiya seismichnykh i aseismichnykh zon* (Nauka, Moscow, 1993), pp. 238–245.
19. A. D. Nozhkin, Yu. M. Puzankov, N. V. Popov, O. M. Turkina, V. I. Berezkin, L. M. Bogomolova, A. N. Zedgenizov, V. I. Kitsul, A. P. Smelov, V. V. Stognii, V. L. Duk, A. B. Kotov, V. I. Medvedev, and A. M. Koveshnikov, "Heat generation in the Earth's crust of the Aldan Shield," in *Temperatura, kriolitozona i radiogennaya teplogeneratsiya v zemnoi kore Severnoi Azii*, Vol. 821 of Tr. OIGGM (Novosibirsk, 1994), pp. 101–112.
20. E. G. Panova, A. P. Kazak, and K. E. Yakobson, "Terrigenous sedimentation in the main Devonian field," Litosfera, No. 4, 19–31 (2003).
21. B. G. Polyak and Ya. B. Smirnov, "Heat flow in the continents," Dokl. Akad. Nauk SSSR **168**, 170–172 (1966).
22. B. G. Polyak and Ya. B. Smirnov, "Relationship between the deep heat flow and the tectonic structure of the continents," Geotektonika, No. 4, 3–19 (1968).
23. B. G. Polyak, I. N. Tolstikhin, and V. P. Yakutseni, "Izotopnyi sostav geliya i teplovoi potok—geokhimicheskii i geofizicheskii aspekty tektogeneza," Geotektonika, No. 5, 3–23 (1979a).
24. B. G. Polyak, E. M. Prasolov, G. I. Buachidze, V. I. Kononov, B. A. Mamyrin, L. I. Surovtseva, L. I. Khabarin, and V. S. Yudenich, "Isotopic distribution of helium and argon isotopes of fluids in the Alpine-Apennine region and its relationship to volcanism," Dokl. Akad. Nauk SSSR **247**, 1220–1225 (1979b).
25. V. E. Sal'nikov, *Geothermal Regime of South Urals* (Nauka, Moscow, 1984) [in Russian].
26. A. A. Smyslov, U. I. Moiseenko, and T. Z. Chadovich, *Thermal Regime and Radioactivity of the Earth* (Nedra, Leningrad, 1979) [in Russian].
27. Ya. B. Smirnov, "Terrestrial heat flow and problems of geosyncline energy," in Vol. 46 of *Tr. Mosk. O-va Ispyt. Prir., Otd. Geol.* (Nauka, Moscow, 1972), pp. 52–74.
28. Ya. B. Smirnov, *Thermal Regime of Tectonosphere: Explanatory Note to the Heat Flow Map of the USSR, 1 : 10000000* (GUGK, Moscow, 1980) [in Russian].
29. *Thermal Field of the Interiors in Siberia*, Ed. by E. E. Fotiady (Nauka, Novosibirsk, 1987) [in Russian].
30. M. D. Khutorskoi, *Geothermics of the Central-Asian Fold Belt* (RUDN, Moscow, 1996) [in Russian].
31. M. D. Khutorskoi, V. A. Golubev, S. V. Kozlovtseva, M. M. Mitnik, and V. V. Yarmolyuk, *Thermal Regime of the Interiors in People Republic of Mongolia* (Nauka, Moscow, 1991) [in Russian].
32. J. F. Albert-Beltran, "Heat flow and temperature gradient data from Spain," in *Terrestrial Heat Flow in Europe* (Springer, Berlin, 1979), pp. 261–266.
33. I. M. Artemieva and W. D. Mooney, "Thermal thickness and evolution of Precambrian lithosphere: A global study," J. Geophys. Res.: Solid Earth **106**, 16387–16414 (2001).
34. L. D. Ashwal, P. Morgan, S. A. Kelly, and J. A. Percival, "Heat production in an Archean crustal profile and implications for heat flow and mobilization of heat-producting elements," Earth Planet. Sci. Lett. **85**, 439–450 (1987).
35. F. Birch, "The present state of geothermal investigation," Geophysics, **19**, 645–659 (1954).
36. F. Birch, R. F. Roy, and E. R. Decker, "Heat flow and thermal history in New England and New York," in *Studies in Appalachian Geology* (New York, 1968), Ch. 33, pp. 437–451.
37. V. Čermak, "Heat flow investigation in Czechoslovakia," in *Geoelectrical and Geothermal Studies (East-Central Europe and Soviet Asia), KAPG Geophys.*

Monogr., Ed. by A. Adam (Akad. Kiado, Budapest, 1976), pp. 414–424.

38. Chapman D. and Pollack H., "Global heat flow: A new look", Planet. Sci. Lett. **28**, 23–32 (1976).
39. S. P. Clark and E. Jaeger, "Denudation rate in the Alps from geochronology date and heat flow date," Am. J. Sci. **267**, 1143–1160 (1969).
40. S. T. Crough and G. A. Thompson, "Thermal model of continental lithosphere," J. Geophys. Res. **81**, 4857–4862 (1976).
41. P. C. England and S. W. Richardson, "The influence of erosion upon the mineral facies of rocks from different metamorphic environments," J. Geol. Soc. London **134**, 201–213 (1977).
42. D. M. Fountain, M. H. Salisbury, and K. P. Furlong, "Heat production and thermal conductivity of rocks from the Pikwitonei-Sachigo continental crust section, central Manitoba: Implication for the thermal structure of Archean crust," Can. J. Earth Sci. **24**, 1583–1594 (1987).
43. K. P. Furlong and D. S. Chapman, "Crustal heterogeneities and the thermal structure of the continental crust," Geophys. Res. Lett. **14**, 314–317 (1987).
44. R. G. Gregory and M. P. Durrance, "Helium, radon and hydrothermal circulation associated with the Carmenwallis radiothermal granite of southwest England," J. Geophys. Res.: Solid Earth **92**, 12567–12586 (1987).
45. V. M. Hamza and R. K. Verma, "The relationship of heat flow with the age of basement rocks," Bull. Volcanol. **33**, 123–152 (1969).
46. D. R. Hilton, E. R. Oxburg, and R. K. O'Nions, "Fluid flow through high heat flow granites: Constraints imposed by He and Rn data," in *High Heat Production (HHP) Granites, Hydrothermal Circulation and Ore Genesis* (Inst. of Min. and Metal., London, 1985), pp. 135–142.
47. D. R. Hilton and H. Craig, "A helium isotope transect along the Indonesian archipelago," Nature **342**, 906–908 (1989).
48. D. R. Hilton, K. Hammerschmidt, S. Teufel, and H. Friedrichsen, "Helium isotope characteristics of Andean geothermal fluids and lavas," Earth. Planet. Sci. Lett. **120**, 265–282 (1993).
49. C. Jaupart and J. C. Mareshal, "Constraints on crustal heat production from heat flow data," in *Treatise on Geochemistry*, Vol. 3: *The Crust*, Ed. by R. L. Rudnick (Pergamon, New York, 2003), pp. 65–84.
50. C. Jaupart, J. G. Sclater, and G. Simmons, "Heat flow studies: Constraints on the distribution of uranium, thorium and potassium in the continental crust," Earth Planet. Sci. Lett. **52**, 328–344 (1981).
51. M. Q. W. Jones, "Heat flow and heat production in the Namaqua mobile belt, South Africa," J. Geophys. Res.: Solid Earth **92**, 6273—6289 (1987).
52. R. A. Ketcham, "Distribution of heat production elements in the upper and middle crust of southern and west central Arizona: Evidence from the core complexes," J. Geophys. Res.: Solid Earth **101**, 13611–13632 (1996).
53. A. H. Lachenbruch, "Preliminary geothermal model of the Sierra Nevada," J. Geophys. Res. **73**, 6977–6989 (1968).
54. A. H. Lachenbruch and J. H. Sass, "Models of an extending lithosphere and heat flow in the Basin and Range province," in *Cenozoic Tectonics and Regional Geophysics*, Vol. 152 of *Geol. Soc. Am., Mem.*, Ed. by R. B. Smith and G. P. Eaton (1978), pp. 209–250.
55. M. K. Lee, G. C. Brown, P. C. Webb, J. Wheildon, and K. E. Rollin, "Heat flow, heat production and thermotectonic setting in mainland UK," J. Geol. Soc., London **144**, 35–42 (1987).
56. J. C. Mareshal, C. Jaupart, and C. Gariepy, "Heat flow and deep thermal structure near the southeastern edge of the Canadian Shield." Can. J. Earth Sci. **37**, 399–414 (2000).
57. D. J. Martel, R. K. O'Nions, D. R. Hilton, and E. R. Oxburgh, "The role of element distribution in production and release of radiogenic helium: The Carmenwallis Granite, Southwestern England," Chem. Geol. **88**, 207–221 (1990).
58. S. M. McLennan and S. R. Taylor, "Heat flow and the chemical composition of continental crust," J. Geol. **104**, 377–396 (1996).
59. P. Morgan and J. H. Sass, "Thermal regime of the continental lithosphere," J. Geodyn. **1**, 143–166 (1984).
60. L. O. Nicolayson, R. J. Hart, and N. H. Gale, "The Vredefort radioelement profile extended to supracrustal strata at Carletonville, with implications for continental heat flow," J. Geophys. Res.: Solid Earth **86**, 10653–10661 (1981).
61. A. A. Nyblade and H. N. Pollack, "A global analysis of heat flow from Precambrian terrains: implications for the thermal structure of Archean and Proterozoic lithosphere," J. Geophys. Res.: Solid Earth **98**, 12207–12218 (1993).
62. F. Parello, P. Allard, W. D'Alessandro, C. Federico, P. Jean-Baptiste, and O. Catani, "Isotope geochemistry of the Panterlleria volcanic fluids, Sicily Channel rift: A mantle volatile end-member for volcanism in southern Europe," Earth. Planet. Sci. Lett. **180**, 325–339 (2000).
63. C. Pinet and C. Jaupart, "The vertical distribution of radiogenic heat production in the Precambrian crust of Norway and Sweden: Geothermal implications," Geophys. Res. Lett. **14**, 260–263 (1987).
64. C. Pinet, C. Jaupart, and J. C. Mareshal, "Heat flow and structure of the lithosphere in the Eastern Canadian shield," J. Geophys. Res.: Solid Earth **96**, 19941–19963 (1991).
65. R. U. M. Rao, G. V. Rao, and G. K. Reddy, "A dependence of continental heat flow – fantasy and facts," Earth. Planet. Sci. Lett. **59**, 288—302 (1982).
66. S. W. Richardson and E. R. Oxburgh, "Heat flow, radiogenic heat production and crustal temperature in England and Wales," J. Geol. Soc. London **135**, 322–327 (1978).
67. R. F. Roy, D. D. Blackwell, and F. Birch, "Heat generation of plutonic rocks and continental heat flow provinces," Earth. Planet. Sci. Lett. **5** 1–12 (1968).
68. R. F. Roy, D. D. Blackwell, and E. R. Decker, "Continental heat flow," in *The Nature of the Solid Earth* (McGraw-Hill, New York, 1972), pp. 506–543.

69. S. Roy and R. U. M. Rao, "Heat flow in the Indian shield," J. Geophys. Res.: Solid Earth **105**, 25587–25604 (2000).

70. L. Royden and K. V. Hodges, "A technique for analyzing the thermal and uplift histories of eroding orogenic belts: A Scandinavian example," J. Geophys. **89**, 7091–7106 (1984).

71. R. L. Rudnick and D. M. Fountain, "Nature and composition of the continental crust: a lower crustal perspective," Rev. Geophys. **33**, 267–309 (1995).

72. R. L. Rudnick, W. F. McDonough, and R. J. O'Connell, "Thermal structure, thickness and composition of continental lithosphere," Chem. Geol. **145**, 395–411 (1998).

73. J. H. Sass, D. D. Blackwell, D. S. Chapman, and S. Roy, "Heat flow of the crust of the United States," in *Physical Properties of Rocks and Minerals* (McGraw-Hill, New York, 1981), pp. 503–548.

74. J. Sclater and J. Francheteau, "The implication of terrestrial heat flow observations on current tectonics and geochemical models of the crust and upper mantle of the earth," Geophys. J. R. Astron. Soc. **20**, 509–542 (1970).

75. J. Sclater, C. Jaupart, and D. Galson, "The heat flow through oceanic and continental crust and the heat loss of the Earth," Rev. Geophys. **18**, 269–311 (1980).

76. J. Sclater, B. Parsons, and C. Jaupart, "Oceans and continents: Similarities and differences in the mechanism and heat flow," J. Geophys. Res.: Solid Earth **86**, 11535–11552 (1981).

77. D. F. Stacey, *Physics of the Earth* (Wiley, New York, 1969).

78. C. A. Swanberg, M. D. Chessman, and G. Simmons, "Heat flow generation studies in Norway," Tectonophysics **23**, 31–48 (1974).

79. H. Y. Tammemagi and J. Wheildon, "Terrestrial heat flow and heat generation in South-West England," Geophys. J. R. Astron. Soc. **38**, 83–94 (1974).

80. I. N. Tolstikhin and J. D. Kramers, *The Evolution of Matter From the Big Bang to Present Day* (Cambridge Univ. Press, Cambridge, 2009).

81. F. J. Turner, *Metamorphic Petrology: Mineralogical and Field Aspects* (McGraw-Hill, New York, 1968).

82. I. Vitorello and H. Pollack, "On the variation of continental heat flow with age and thermal evolution of continents," J. Geophys. Res.: Solid Earth **85**, 983–995 (1980).

83. B. L. Weaver and J. Tarney, "Empirical approach to estimating the composition of the continental crust," Nature **59**, 575–577 (1984).

84. P. C. Webb, A. G. Tindle, S. D. Barritt, G. C. Brown, and J. F. Miller, "Radiothermal granites in the United Kingdom," in *High Heat Production (HHP) Granites, Hydrothermal Circulation and Ore Genesis* (Inst. of Min. and Metal., London, 1985), pp. 409–424.

85. J. Wheildon, M. F. Francis, J. R. L. Ellis, and A. Thomas-Betts, "Exploration and interpretation of the SW England geothermal anomaly," in *Proceedings of 2nd International Seminar on Results of EC Geothermal Energy Resources, Strasbourg, 1980*, Ed. by A. S. Strub and P. Ungemach, (Comm. Eur. Communities, Strasbourg, 1980), pp. 456–463.

Reviewer: E.A. Rogozhin

Translated by V. Popov